Journal of Cerebral Blood Flow & Metabolism (2013) 33, 1523–1531

www.jcbfm.com

ORIGINAL ARTICLE

# Glutamatergic and GABAergic TCA cycle and neurotransmitter cycling fluxes in different regions of mouse brain

Vivek Tiwari, Susmitha Ambadipudi and Anant B Patel

The $^{13}C$ nuclear magnetic resonance (NMR) studies together with the infusion of $^{13}C$-labeled substrates in rats and humans have provided important insight into brain energy metabolism. In the present study, we have extended a three-compartment metabolic model in mouse to investigate glutamatergic and GABAergic tricarboxylic acid (TCA) cycle and neurotransmitter cycle fluxes across different regions of the brain. The $^{13}C$ turnover of amino acids from [1,6-$^{13}C_2$]glucose was monitored *ex vivo* using $^{1}H$-[$^{13}C$]-NMR spectroscopy. The astroglial glutamate pool size, one of the important parameters of the model, was estimated by a short infusion of [2-$^{13}C$]acetate. The ratio $V_{cyc}/V_{TCA}$ was calculated from the steady-state acetate experiment. The $^{13}C$ turnover curves of [4-$^{13}C$]/[3-$^{13}C$]glutamate, [4-$^{13}C$]glutamine, [2-$^{13}C$]/[3-$^{13}C$]GABA, and [3-$^{13}C$]aspartate from [1,6-$^{13}C_2$]glucose were analyzed using a three-compartment metabolic model to estimate the rates of the TCA cycle and neurotransmitter cycle associated with glutamatergic and GABAergic neurons. The glutamatergic TCA cycle rate was found to be highest in the cerebral cortex ($0.91 \pm 0.05$ $\mu$mol/g per minute) and least in the hippocampal region ($0.64 \pm 0.07$ $\mu$mol/g per minute) of the mouse brain. In contrast, the GABAergic TCA cycle flux was found to be highest in the thalamus–hypothalamus ($0.28 \pm 0.01$ $\mu$mol/g per minute) and least in the cerebral cortex ($0.24 \pm 0.02$ $\mu$mol/g per minute). These findings indicate that the energetics of excitatory and inhibitory function is distinct across the mouse brain.

*Journal of Cerebral Blood Flow & Metabolism* (2013) **33,** 1523–1531; doi:10.1038/jcbfm.2013.114; published online 10 July 2013

**Keywords:** GABA; glutamate; neuron-glia trafficking; regional metabolism; neurotransmitter cycle; nuclear magnetic resonance spectroscopy

## INTRODUCTION

Glutamate (Glu) and gamma-aminobutyric acid (GABA) are the most abundant neurotransmitters in the cerebral cortex and are responsible for the excitatory and inhibitory neurotransmissions in the matured central nervous system. These neurotransmitters are involved in many functions such as motor behavior, cognition, and emotion.[1,2] Perturbation in glutamatergic and GABAergic neurotransmission is associated with several neurological and psychiatric disorders.[3] *In vivo* $^{13}C$ nuclear magnetic resonance (NMR) studies in rat and human brain have established that the Glu-glutamine (Gln) cycle accounts for a major fraction ($>80\%$) of Gln synthesis. Experiments conducted in the rat brain under conditions of graded anesthesia have shown that rates of neurotransmitter cycle and neuronal glucose oxidation are stoichiometrically coupled through the entire level of brain activity, thus indicating that neurotransmitter energetics is supported by oxidative glucose metabolism.[4,5] $^{13}C$ NMR studies in the rat brain have indicated that GABA also contributes significantly to neuronal glucose oxidation and neurotransmitter cycling flux.[4,6]

Extensive $^{13}C$ NMR studies of cerebral metabolism in rat[4,5,7–10] and human[11–13] brain have given important insights into neurotransmitter energetics. *In vivo* $^{13}C$ NMR and autoradiography studies conducted in rat brain indicated that metabolism is not uniform across the brain.[7,14,15] Successful completion of the human genome project led to the development of transgenic models of various cerebral disorders in mice. However, cerebral metabolism in mice has not been understood quantitatively. The understanding of regional energetics of glutamatergic and GABAergic neurotransmission in normal mice is indispensible to gain insight into the pathophysiology of various human neurological disorders using transgenic mouse models.

In the present study, we have extended the three-compartment metabolic model[4] in mice to investigate glutamatergic and GABAergic fluxes in cerebral cortex (Cx), hippocampus (Hip), striatum (Str), thalamus–hypothalamus (THt), and cerebellum (Cb) regions. The $^{13}C$ turnover of amino acids from [1,6-$^{13}C_2$]glucose was measured *ex vivo* using $^{1}H$-[$^{13}C$]-NMR spectroscopy. The astroglial Glu pool size was estimated using a short-time infusion of [2-$^{13}C$]acetate. The ratio $V_{cyc}/V_{TCA}$ for glutamatergic and GABAergic neurons was measured from the steady-state [2-$^{13}C$]acetate measurement. The $^{13}C$ turnover of cerebral amino acids from [1,6-$^{13}C_2$]glucose was analyzed using a three-compartment metabolic model to determine metabolic rates associated with the glutamatergic and GABAergic pathway in different regions of the mouse brain. Our findings indicate that the glucose oxidation and neurotransmitter cycling fluxes of glutamatergic and GABAergic neurons vary across the different regions in the mouse brain.

## MATERIALS AND METHODS

### Animal Preparation

All experiments were conducted in accordance with the protocols approved by Institutional Animal Ethics Committee of CCMB. ARRIVE

NMR Microimaging and Spectroscopy, CSIR-Centre for Cellular and Molecular Biology, Habsiguda India. Correspondence: Dr AB Patel, NMR Microimaging and Spectroscopy, CSIR-Centre for Cellular and Molecular Biology, Uppal Road, Habsiguda, Hyderabad 500 007, India.
E-mail: abpatel@ccmb.res.in
All NMR experiments were performed at NMR Facility, CCMB, Hyderabad, India. VT gratefully acknowledges the Senior Research Fellowship from CSIR. This study was supported by fundings from DBT BT/PR14064/Med/30/359/2010 and CSIR network project BSC0208 to ABP.
Received 20 March 2013; revised 22 May 2013; accepted 14 June 2013; published online 10 July 2013

guidelines were followed in the preparation of the manuscript. Thirty-five male C57BL6 (2 months old) mice were fasted for 12 hours before infusion of $^{13}$C-labeled substrates. Mice were anesthetized with urethane (1.5 g/kg, intraperitoneally). Core body temperature of the animal was measured using a rectal probe and maintained at $\sim 37^{\circ}$C by placing it supine on a heating pad connected to a temperature-regulated circulating water bath. The tail vein was cannulated for infusion of $^{13}$C-labeled glucose or acetate. Animal respiration was monitored throughout the experiment by using the BIOPAC device (Santa Barbara, CA, USA) interfaced to a computer.

### Infusion of [1,6-$^{13}C_2$]Glucose and [2-$^{13}$C]Acetate

A solution of [1,6-$^{13}C_2$]glucose (99 atom%, Cambridge isotope, Andover, MA, USA) was infused in mice through the tail vein for 7, 15, 30, 60, and 90 minutes ($n = 5$ for each time point) after 45 minutes of urethane anesthesia. The [1,6-$^{13}C_2$]glucose (0.225 mol/L) dissolved in deionized water was delivered as a bolus for the first 15 seconds, followed by an exponentially decreasing infusion rate every 30 seconds for the next 8 minutes, whereupon the infusion rate was constant until *in situ* brain freezing.[16] The infusion rate of [1,6-$^{13}C_2$]glucose at steady state ($\geqslant$8.25 minutes) was 15 $\mu$mol/kg per minute. [2-$^{13}$C]acetate (1 mol/L) and unlabeled glucose (0.225 mol/L), dissolved in deionized water and pH adjusted to 7.0, were administered to mice ($n = 5$) by bolus-variable infusion rate as described previously.[9] The [2-$^{13}$C]acetate infusion rate was 0.2 mmol/kg per minute at the steady state. The infusion was terminated at 90 minutes, which was sufficient to attain the steady-state $^{13}$C enrichments of $Glu_{C4}$, $GABA_{C2}$, and $Gln_{C4}$. In addition, mice ($n = 5$) were also infused with [2-$^{13}$C]acetate for 3 minutes to estimate the size of astroglial Glu pool. Blood was collected from sinus orbitus using the fine capillary just before the termination of infusion. Plasma was collected after centrifugation of the blood and stored at $-80^{\circ}$C for subsequent analysis. At the end of the infusion, mouse brain was frozen *in situ* using liquid $N_2$.

### Preparation of Brain Extracts for Nuclear Magnetic Resonance Analysis

The mouse brain was dissected in a cryostat (maintained at $-20^{\circ}$C) to isolate cerebellum, cerebral cortex, hippocampus, striatum, and thalamus–hypothalamus regions. Metabolites were extracted from frozen tissue as described previously.[17] In brief, the frozen tissue was weighed (Supplementary Table 2S) and powdered with 0.1 N HCl in methanol (1:2 w/v) in a dry ice/ethanol bath. The [2-$^{13}$C]glycine (100 $\mu$l; 2 mmol/L) was added as an internal concentration reference. The tissue powder was thoroughly homogenized with ice-cold ethanol (1:6 w/v; 60% ethanol), and the homogenate was clarified by centrifugation at 20,000 *g*. The tissue extract was passed through the chelex column, and the pH of the extract was adjusted to 7.0. The extract was lyophilized and dissolved in phosphate-buffered (50 mmol/L, pH = 7.0) deuterium oxide containing sodium 3-trimethylsilyl[2,2,3,3-D4]-propionate (TSP) (0.5 mmol/L) as a chemical shift reference.

The brain extracts obtained from short-time infusion of [2-$^{13}$C]acetate were passed through an AG 1-X8 anion exchange column to separate Gln and Glu. Gln and neutral molecules were eluted using deionized water, whereas Glu and anionic molecules were eluted using 2 mol/L acetic acid.[17] Both fractions were lyophilized and resuspended in a phosphate-buffered (50 mmol/L, pH = 7) deuterium oxide solution containing 0.5 mmol/L TSP for further $^1$H-[$^{13}$C]-NMR analysis.

### Nuclear Magnetic Resonance Analysis of Brain Extract and Plasma

All NMR measurements were carried out on a 600-MHz (Bruker Biospin, Rheinstetten, Germany) spectrometer. The $^1$H-[$^{13}$C]-NMR spectra of tissue extracts were acquired using a pulse sequence that incorporates adiabatic pulses for $^1$H and $^{13}$C frequencies.[16,18] Concentrations of metabolites were determined relative to [2-$^{13}$C]glycine, added during tissue extraction as an internal concentration reference. The concentration thus obtained represents weighted average of gray matter, white matter, and cerebrospinal fluid in the given brain region. The $^{13}$C atom percent enrichment of metabolites at different carbon positions was determined as the ratio of the peak areas in the $^1$H-[$^{13}$C]-NMR difference spectrum ($2 \times {}^{13}$C only) to the nonedited spectrum ($^{12}C + {}^{13}C$). The percent enrichment of metabolites was corrected for $^{13}$C natural abundance by subtraction of 1.1%.

Blood plasma was mixed with deuterium oxide containing 0.5 mmol/L sodium formate and passed through a centrifugal filter (10-kDa cut off) to remove macromolecules. Plasma samples were analyzed using $^1$H NMR spectroscopy to determine the total concentration and $^{13}$C enrichment of glucose and acetate. Water resonance was suppressed by continuous irradiation during the relaxation delay. The concentration of glucose and acetate was determined using formate as reference. The isotopic $^{13}$C enrichment of glucose-C1$\alpha$ (5.2 p.p.m.) and acetate-C2 (1.9 p.p.m.) was calculated by dividing the areas of the $^{13}$C satellites with the total area ($^{12}C + {}^{13}C$).

### Determination of Glutamate Pool in Neurons and Astroglia

Astroglial Glu pool size, which is required for the three-compartment metabolic modeling, is not established across different regions of the mouse brain. The pool size of Glu in astroglia was estimated by using a very short-time infusion of [2-$^{13}$C]acetate. The measured Glu labeling from [2-$^{13}$C]acetate is the weighted average of neuronal and astroglial fraction:

$$Glu_{C4(obs)} = fxGlu_{C4(g)} + (1-f)xGlu_{C4(n)} \quad \text{Equation (1)}$$

where $Glu_{C4(g)}$ and $Glu_{C4(n)}$ are the percent $^{13}$C enrichment of astroglial and neuronal Glu pool, and '*f* ' is the fraction of astroglial Glu. As astroglial Glu is the precursor for Gln and $Glu_{C4(g)} \sim Gln_{C4}$ for a short-time infusion of [2-$^{13}$C]acetate, $Glu_{C4(n)} \sim 0$. Hence, Equation (1) is reduced to the following:

$$f = \frac{Glu_{C4(obs)}}{Gln_{C4}} \quad \text{Equation (2)}$$

### Determination of $V_{cyc}/V_{TCA}$ from [2-$^{13}$C]Acetate Studies

The ratio of $V_{cyc}/V_{TCA}$ for glutamatergic and GABAergic neurons was calculated in different regions of the brain by steady-state labeling of $Glu_{C4}$, $GABA_{C2}$, and $Gln_{C4}$ from [2-$^{13}$C]acetate.[4] For glutamatergic neurons, the ratio of Glu–Gln cycle to glutamatergic TCA cycle fluxes ($V_{cyc(Glu\text{-}Gln)}/V_{TCA(Glu)}$) was calculated using the following equation:

$$\frac{V_{cyc(Glu-Gln)}}{V_{TCA(Glu)}} = \frac{Glu_{C4}}{Gln_{C4} - Glu_{C4}} \quad \text{Equation (3)}$$

where $Glu_{C4}$ and $Gln_{C4}$ are the labeling of neuronal [4-$^{13}$C]glutamate and astroglial [4-$^{13}$C]glutamine, respectively, from [2-$^{13}$C]acetate at the steady state. Glutamine and GABA were assumed to be entirely localized in astroglia and GABAergic neurons, respectively, whereas Glu was distributed in glutamatergic neurons, GABAergic neurons, and astroglia

**Table 1.** Astroglial Glu pool and $V_{cyc}/V_{TCA}$ in different regions of mouse brain

| | *3 minutes* | | *90 minutes* | | | | $V_{cyc}/V_{TCA}$ | |
|---|---|---|---|---|---|---|---|---|
| *Brain region* | $Glu_{C4}$ | $Gln_{C4}$ | $Glu_{C4}$ | $GABA_{C2}$ | $Gln_{C4}$ | $fGlu_a$ | *Glutamatergic* | *GABAergic* |
| Cx | 0.54 ± 0.07 | 3.23 ± 0.35 | 7.2 ± 0.1 | 5.7 ± 0.35 | 15.3 ± 1.1 | 0.16 ± 0.01 | 0.39 ± 0.04 | 0.43 ± 0.02 |
| Hip | 0.43 ± 0.16 | 3.6 ± 0.63 | 6.0 ± 1.1 | 4.1 ± 0.7 | 13.3 ± 1.6 | 0.12 ± 0.04 | 0.49 ± 0.03 | 0.35 ± 0.02 |
| Str | 0.46 ± 0.13 | 3.06 ± 0.5 | 5.0 ± 0.7 | 4.5 ± 0.7 | 13.5 ± 2.0 | 0.15 ± 0.04 | 0.24 ± 0.03 | 0.43 ± 0.02 |
| THt | 0.59 ± 0.14 | 4.52 ± 0.17 | 5.8 ± 0.8 | 5.3 ± 0.3 | 14.5 ± 1.2 | 0.13 ± 0.03 | 0.30 ± 0.03 | 0.44 ± 0.03 |
| Cb | 0.26 ± 0.06 | 2.90 ± 0.53 | 6.6 ± 0.6 | 4.9 ± 0.8 | 15.1 ± 1.7 | 0.09 ± 0.01 | 0.40 ± 0.03 | 0.33 ± 0.02 |

Abbreviations: Cb, cerebellum; Cx, cortex; Hip, hippocampus; Str, striatum; THt, thalamus–hypothalamus.
Astroglial Glu pool size ($fGlu_a$) was estimated by using Equation (2) and $^{13}$C labeling of amino acids obtained during a short-time infusion (3 minutes) of [2-$^{13}$C]acetate. The ratio, $V_{cyc}/V_{TCA}$ for glutamatergic and GABAergic neurons was estimated using Equations (3) and (4), and labeling of amino acids from [2-$^{13}$C]acetate at steady state (90 minutes). All values are presented as mean ± s.d.

in the ratio 82:2:16 in cerebral cortex, as determined using Equation (2) (Table 1). Enrichment of neuronal [4-$^{13}$C]glutamate was calculated under the assumption that at the steady state $^{13}$C enrichment of astroglial Glu is equal to Gln. The $^{13}$C Labeling of amino acids from [1-$^{13}$C]/[6-$^{13}$C]glucose generated from [2-$^{13}$C]acetate via gluconeogenesis was corrected by subtracting the [3-$^{13}$C]lactate enrichment.

Similarly, the ratio of GABA-Gln cycle to GABAergic TCA cycle ($V_{cyc(GABA-Gln)}/V_{TCA(GABA)}$) was calculated as follows:

$$\frac{V_{cyc(GABA-Gln)}}{V_{TCA(GABA)}} = \frac{GABA_{C2}}{Gln_{C4} - GABA_{C2}} \quad \text{Equation (4)}$$

where $GABA_{C2}$ is the steady-state $^{13}$C labeling of [2-$^{13}$C]GABA from [2-$^{13}$C]acetate.

### Determination of Metabolic Rates

The $^{13}$C turnover of amino acids from [1,6-$^{13}C_2$]glucose was constructed using the measured $^{13}$C labeling in tissue extract for different infusion times. Metabolic rates were determined by fitting a three-compartment metabolic model (Figure 1; glutamatergic neurons, GABAergic neurons, and astroglia) to the $^{13}$C turnover of $Glu_{C4}$, $Glu_{C3}$, $GABA_{C2}$, $GABA_{C3}$, $Gln_{C4}$, and $Asp_{C3}$ from [1,6-$^{13}C_2$]glucose.[4] The metabolic model consists of a series of coupled differential equations reflecting mass balance and $^{13}$C isotope flowing from [1,6-$^{13}C_2$]glucose (Supplementary Table 1S) into neuronal and astroglial amino acids using the CWave software package executed in Matlab (Mathworks, Natick, MA, USA).[19] The mass and isotope balance equations for the three-compartment metabolic model were similar to those described previously in detail.[4] The differential equations were solved using the Runge–Kutta algorithm, and the fitting was done using a Levenberg–Marquardt algorithm.[20] The cerebral metabolic fluxes were determined from the best fits of the model to the $^{13}$C turnover data. In the case of the cerebral cortex, Glu pool was distributed among glutamatergic neurons (82%), GABAergic neurons (2%), and astroglia (16%) (Table 1). The ratios $V_{cyc(Glu-Gln)}/V_{TCA(Glu)}$ and $V_{cyc(GABA-Gln)}/V_{TCA(GABA)}$ obtained from Equations 3 and 4 were used as constraints to relate the $V_{cyc}$ to $V_{TCA}$ when fitting the model to $^{13}$C turnover of cerebral amino acids from [1,6-$^{13}C_2$]glucose. The uncertainties in metabolic rates were obtained by Monte Carlo analysis, where 25 values of each rates were obtained by fitting the model to the randomly generated $^{13}$C turnover curve of amino acids.

### Statistical Analysis

The statistical significance of differences for metabolite levels and metabolic rates among different brain regions was determined using analysis of variance. All results are presented as mean ± s.d.

## RESULTS

### Plasma Glucose and Acetate Level and Enrichment

Infusion of [1,6-$^{13}C_2$]glucose led to a rapid increase in total glucose level from 8.8 ± 0.7 mmol/L to 15.9 ± 1.7 mmol/L within 7 minutes and remained elevated during the entire course of experiment. The $^{13}$C enrichment of glucose-C1 also increased rapidly to 37.9% in 7 minutes, and thereafter remained at ~40% throughout the infusion of [1,6-$^{13}C_2$]glucose. Plasma acetate level and $^{13}$C enrichment were found to be 3.7 ± 0.8 mmol/L and 81.2 ± 5.2%, respectively, after 90 minutes of [2-$^{13}$C]acetate infusion.

### Level of Metabolites in Different Regions of the Mouse Brain

Metabolite levels in different brain regions were measured from nonedited $^1$H-[$^{13}$C]-NMR spectrum (Figure 2 upper panel). The levels of metabolites were found to vary across the brain and were distinct in the different regions of the brain (Figure 3). The levels of Glu (13.8 ± 0.1 μmol/g) and N-acetylaspartate (NAA) (8.1 ± 0.2 μmol/g) were highest in the cerebral cortex. However, the level of GABA was highest in the thalamus–hypothalamus (4.3 ± 0.1 μmol/g) and least in the cerebellum (2.3 ± 0.1 μmol/g). The level of inositol was higher in the thalamus–hypothalamus (8.4 ± 0.2 μmol/g) and striatum (8.3 ± 0.3 μmol/g) and least in the cerebral cortex (6.5 ± 0.2 μmol/g). Glutamine level was highest in the cerebral cortex (5.5 ± 0.1 μmol/g) and lowest in the striatum (4.8 ± 0.1 μmol/g).

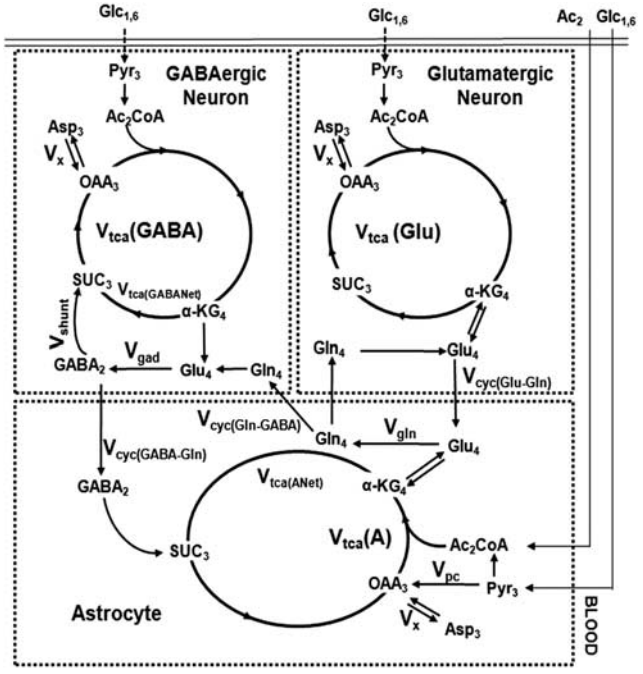


**Figure 1.** A three-compartment metabolic model showing the $^{13}$C labeling of cerebral metabolites from [1,6-$^{13}C_2$]glucose and [2-$^{13}$C]acetate. Although [1,6-$^{13}C_2$]glucose is metabolized in the neurons and astroglia, [2-$^{13}$C]acetate is selectively transported and metabolized in astroglia. Metabolism of [1,6-$^{13}C_2$]glucose via glutamatergic and GABAergic tricarboxylic acid (TCA) cycle labels $Glu_{C4}$. In GABAergic neurons, $Glu_{C4}$ is decarboxylated to $GABA_{C2}$. Labeling of $Gln_{C4}$ occurs from $Glu_{C4}$ and $GABA_{C2}$ via Glu–Gln and GABA-Gln cycle, respectively. Further metabolism in the TCA cycle labels $Glu_{C2/3}$, $Gln_{C2/3}$, $GABA_{C3/4}$, and $Asp_{C2/3}$. The [2-$^{13}$C]acetate metabolism in astroglia labels $Gln_{C4}$ by combined action of astroglial TCA cycle and glutamine synthetase activity. $Glu_{C4}$ and $GABA_{C2}$ are labeled from $Gln_{C4}$ via Glu–Gln and GABA-Gln substrates cycling, respectively, between astroglia and neurons. Subsequent metabolism through TCA cycle incorporates labels into $Glu_{C2/3}$, $Gln_{C2/3}$, $GABA_{C3/4}$, and $Asp_{C2/3}$ $V_{cyc(GABA-Gln)}$, GABA-Gln cycling flux; $V_{cyc(Glu-Gln)}$, Glu–Gln cycling flux; $V_{gad}$, glutamate decarboxylase flux; $V_{gln}$, rate of glutamine synthesis; $V_{pc}$, pyruvate carboxylase flux; $V_{shunt}$, flux of GABA shunt; $V_{TCA(A)}$, astroglial TCA cycle flux; $V_{TCA(GABA)}$, GABAergic TCA cycle flux; $V_{TCA(Glu)}$, glutamatergic TCA cycle flux.

### Labeling of Cerebral Amino Acids from [1,6-$^{13}C_2$]Glucose and [2-$^{13}$C]Acetate

Typical $^1$H-[$^{13}$C]-NMR spectra obtained from the cerebral cortex of the mouse infused with either [1,6-$^{13}C_2$]glucose or [2-$^{13}$C]acetate for 90 minutes are shown in Figure 2. The $^{13}$C intensity of amino acids from [1,6-$^{13}C_2$]glucose (Figure 2A lower panel) is much higher than that of [2-$^{13}$C]acetate (Figure 2B lower panel), thus suggesting glucose as the preferred energy substrate over acetate in the brain. Further, the magnitude of labeling of $Glu_{C4}$ and $Gln_{C4}$ from [2-$^{13}$C]acetate is opposite to that of [1,6-$^{13}C_2$]glucose. In the cerebral cortex, $^{13}$C enrichment of $Gln_{C4}$ (15.3 ± 1.1%) was found to be significantly higher than $Glu_{C4}$ (7.2 ± 0.1%) and $GABA_{C2}$ (5.7 ± 0.3%) in [2-$^{13}$C]acetate experiment, whereas labeling of $Gln_{C4}$ (23.6 ± 0.5%) was lower than $Glu_{C4}$ (36.1 ± 0.5%) and $GABA_{C2}$ (29.6 ± 1.1%) in [1,6-$^{13}C_2$]glucose experiment (Supplementary

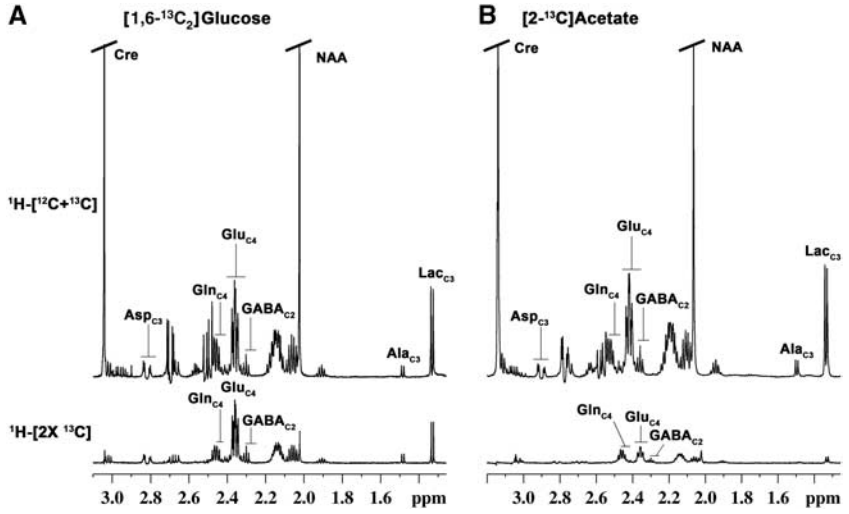


**Figure 2.** Typical $^{1}$H-[$^{13}$C]-nuclear magnetic resonance (NMR) spectra from cortical tissue extract prepared after 90 min of (**A**) [1,6-$^{13}C_2$]glucose and (**B**) [2-$^{13}$C]acetate infusion. Upper panel, nonedited $^{1}$H-[$^{12}C + {}^{13}$C] spectrum represents total concentration of neurometabolites. The lower panel represents $^{13}$C-edited spectrum showing labeling from [1,6-$^{13}C_2$]glucose (left panel) and [2-$^{13}$C]acetate (right panel). Peak labeling is as follows: $Ala_{C3}$, alanine-C3; $Asp_{C3}$, aspartate-C3; $GABA_{C2}$, GABA-C2; $Gln_{C4}$, glutamine-C4; $Glu_{C4}$, glutamate-C4.

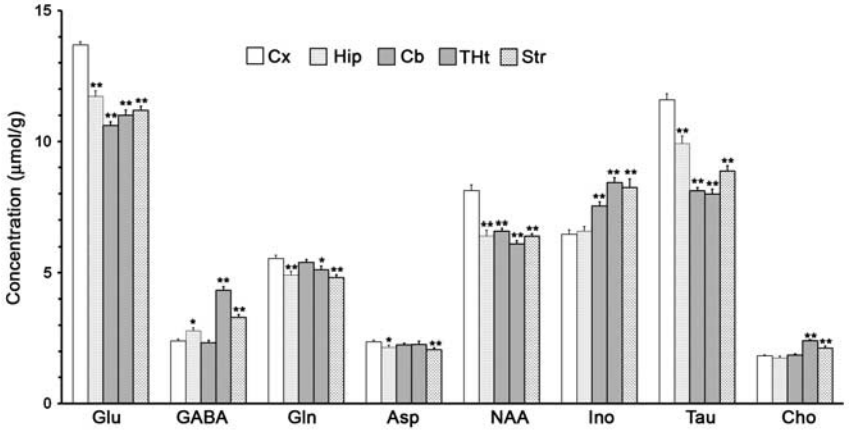


**Figure 3.** Metabolite concentration ($\mu$mol/g) in different brain regions. The concentration of metabolites was determined from $^{1}$H-[$^{13}C + {}^{12}$C]-nuclear magnetic resonance spectrum using [2-$^{13}$C]glycine as the internal reference. The values are mean ± s.e.m. ($n = 25$). *$P < 0.05$, **$P < 0.001$ when compared with respective cortical value.

Table 2S). Moreover, labeling of amino acids from glucose was observed to be higher than acetate. The higher labeling of $Gln_{C4}$ than $Glu_{C4}$ from [2-$^{13}$C]acetate is in accordance with the preferential utilization of acetate in astrocytes, whereas higher labeling of $Glu_{C4}$ and $GABA_{C2}$ over $Gln_{C4}$ from glucose suggests preferential utilization of glucose by neurons.

Spectral time course of $^{13}$C labeling of cortical amino acids from [1,6-$^{13}C_2$]glucose is shown in Figure 4. Early-time-point infusion spectra (7 and 15 minutes) show well-resolved signals from $Glu_{C4}$ and $GABA_{C2}$, which are labeled via the first turn of the TCA cycle; furthermore, later-time-point spectra (30, 60, and 90 minutes) exhibited signals from $Glu_{C3}$, $Asp_{C3}$, $GABA_{C3}$, and $GABA_{C4}$, which are labeled in the subsequent turn of the TCA cycle. Spectral time course displayed well-resolved signals from $Glu_{C4,C3}$, $Gln_{C4}$, $GABA_{C2,C3,C4}$, and $Asp_{C3}$, which increased with time. The $^{13}$C turnover of amino acids from [1,6-$^{13}C_2$]glucose at different carbon positions, constructed by plotting the normalized $^{13}$C enrichment of amino acids with plasma glucose enrichment with time, was used for metabolic flux analysis.

## Glutamate Pool Distribution in Neurons and Astroglia

Glutamatergic and GABAergic TCA cycle and neurotransmitter cycle fluxes in different regions of the mouse brain were evaluated by fitting a three-compartment metabolic model (Figure 1; Supplementary Table 1S) to the $^{13}$C turnover of amino acids from [1,6-$^{13}C_2$]glucose. One of the important parameters in the model is the astroglial Glu pool size, which is not established in different regions of the mouse brain. Astroglial Glu pool was estimated from a short infusion of [2-$^{13}$C]acetate and was found to vary from 9% to 16% in different regions of the mouse brain (Table 1). Astroglial Glu pool was found to be highest in the cerebral cortex (16%) and least in the cerebellum (9%), whereas other regions (hippocampus 12%; thalamus–hypothalamus 13%; striatum 15%) showed an intermediate value.

## Glutamatergic and GABAergic Fluxes

The ratio of $V_{cyc}/V_{TCA}$ for glutamatergic and GABAergic neurons for different regions of the mouse brain was calculated using Equations 3 and 4, respectively, from the steady-state $^{13}$C labeling

of amino acids from [2-$^{13}$C]acetate (Table 1). The ratio $V_{cyc}/V_{TCA}$ for glutamatergic neurons was found to be highest for the hippocampus (0.49 ± 0.03) and least for the striatum (0.24 ± 0.03) (Table 1). For GABAergic neuron, $V_{cyc}/V_{TCA}$ was higher in the thalamus–hypothalamus (0.44 ± 0.03), cortex (0.43 ± 0.02), and striatum (0.43 ± 0.03), and lowest in the cerebellum (0.33 ± 0.02).

The fit of the metabolic model to $^{13}$C turnover of amino acids in the cerebral cortex is depicted in Figure 5. The random distribution of residual together with low value of the least-square standard deviation between measured and predicted turnover suggests a good fit of the model to the measured data. The quality of the fit of the model to $^{13}$C turnover of amino acids was similar for other brain regions, as revealed by similar least-square standard deviation. The glutamatergic TCA cycle rate in the cerebral cortex (0.91 ± 0.05 μmol/g per minute) was observed to be significantly higher ($F[1,48] = 231$, $P = 5.3e\text{-}^{20}$) than other brain regions (Figure 6, Supplementary Table 3S). The TCA cycle flux decreased in the order of cerebral cortex > cerebellum (0.81 ± 0.09 μmol/g per minute) > striatum (0.75 ± 0.05 μmol/g per minute) ~ thalamus–hypothalamus (0.73 ± 0.05 μmol/g per minute) > hippocampus (0.64 ± 0.07 μmol/g per minute). The Glu–Gln cycle rate was higher ($F[1,48] = 14$, $P = 0.0004$) in the cerebral cortex (0.36 ± 0.02 μmol/g per minute) as compared with the other regions. The glutamatergic neurotransmitter cycle rate was in the following order: cerebral cortex > cerebellum (0.32 ± 0.04 μmol/g per minute) ~ hippocampus (0.31 ± 0.04 μmol/g per minute) > thalamus–hypothalamus (0.22 ± 0.02 μmol/g per minute) > striatum (0.18 ± 0.01 μmol/g per minute).

The GABAergic TCA cycle flux was significantly ($F[1,48] = 5.2$, $P = 0.026$) higher in the thalamus–hypothalamus (0.28 ± 0.01 μmol/g per minute) than in other brain regions. The $V_{TCA(GABA)}$ decreased in the following order: thalamus–hypothalamus > striatum (0.27 ± 0.02 μmol/g per minute) > hippocampus (0.26 ± 0.04 μmol/g per minute) > cerebellum (0.25 ± 0.03 μmol/g per minute) > cerebral cortex (0.24 ± 0.02 μmol/g per minute) (Figure 6, Supplementary Table 3S). The rate of GABA-Gln cycle in the thalamus–hypothalamus (0.12 ± 0.01 μmol/g per minute) was found to be significantly ($F[1,48] = 11.89$, $P = 0.0011$) higher than that in other brain regions. The GABAergic neurotransmission decreased in the following order: thalamus–hypothalamus > striatum (0.11 ± 0.01 μmol/g per minute) > cerebral cortex (0.10 ± 0.01 μmol/g per minute) > hippocampus (0.09 ± 0.01 μmol/g per minute) > cerebellum (0.08 ± 0.01 μmol/g per minute). The astroglial TCA cycle flux ($V_{TCA(A)}$) was also found to vary across the different regions of the brain in the following order: cerebellum (0.28 ± 0.03 μmol/g per minute) > hippocampus (0.26 ± 0.05 μmol/g per minute) ~ thalamus–hypothalamus (0.26 ± 0.01 μmol/g per minute) ~ cerebral cortex (0.25 ± 0.03 μmol/g per minute) > striatum (0.19 ± 0.02 μmol/g per minute).

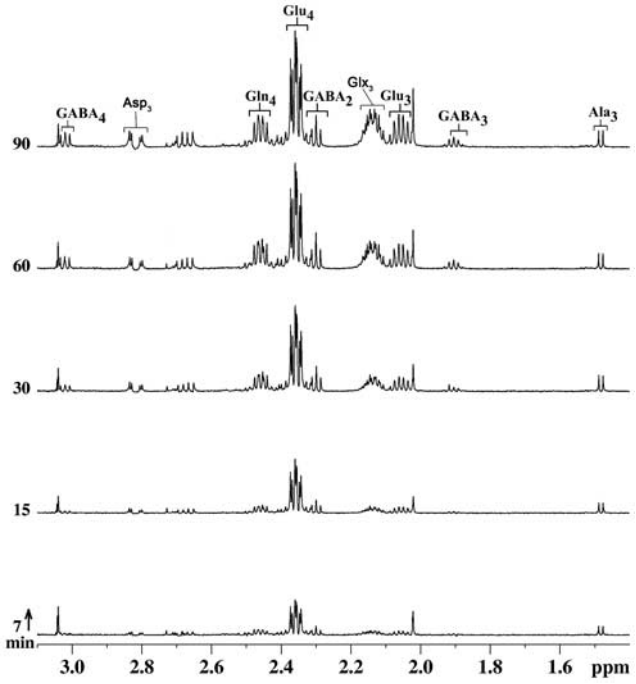


**Figure 4.** Representative $^{1}$H-[$^{13}$C]-nuclear magnetic resonance (NMR) spectra of cortical extract with time showing the $^{13}$C labeling of cortical metabolites from [1,6-$^{13}C_2$]glucose. Mice were infused with [1,6-$^{13}C_2$]glucose for a predefined duration, and $^{1}$H-[$^{13}$C]-NMR spectra were recorded from cortical tissue extracts. Peak labeling is the same as in Figure 3.

## DISCUSSION

The current study provides, for the first time, the quantitative fluxes associated with different metabolic pathways across the

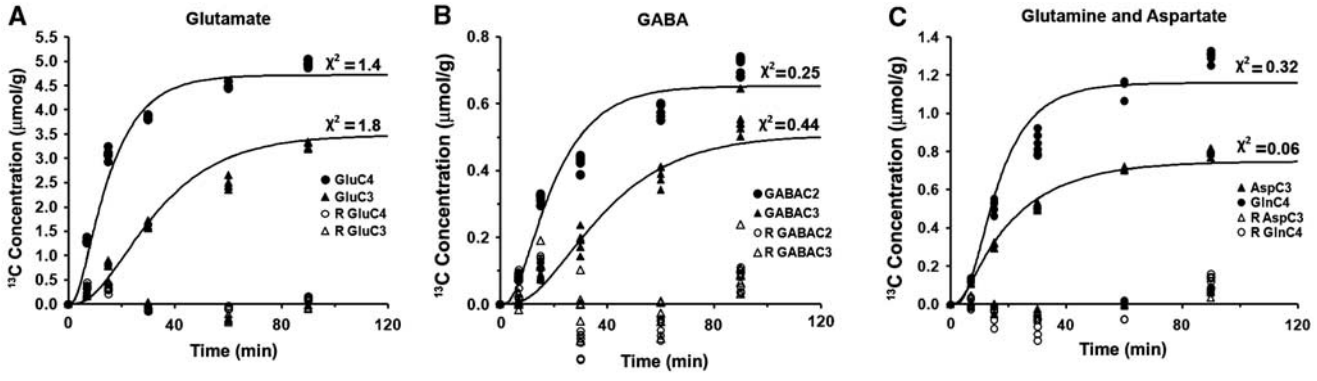


**Figure 5.** The fit of the metabolic model to the $^{13}$C turnover of cortical (**A**) GluC4 and GluC3, (**B**) GABAC2 and GABAC3, (**C**) GlnC4 and AspC3 from [1,6-$^{13}C_2$]glucose. Mice were infused with [1,6-$^{13}C_2$]glucose for a predefined duration. The $^{13}$C enrichment of cortical amino acids was measured in extract using $^{1}$H-[$^{13}$C]-nuclear magnetic resonance spectroscopy. The $^{13}$C concentration was obtained by multiplying the total concentration with corresponding $^{13}$C enrichment. Residual (R) between measured and fitted time course was obtained as follows: (measured − calculated) × (calculated)$^{-1/2}$. Symbols represent the measured $^{13}$C labeling, whereas lines show the best fit of the three-compartment metabolic model to the measured data.

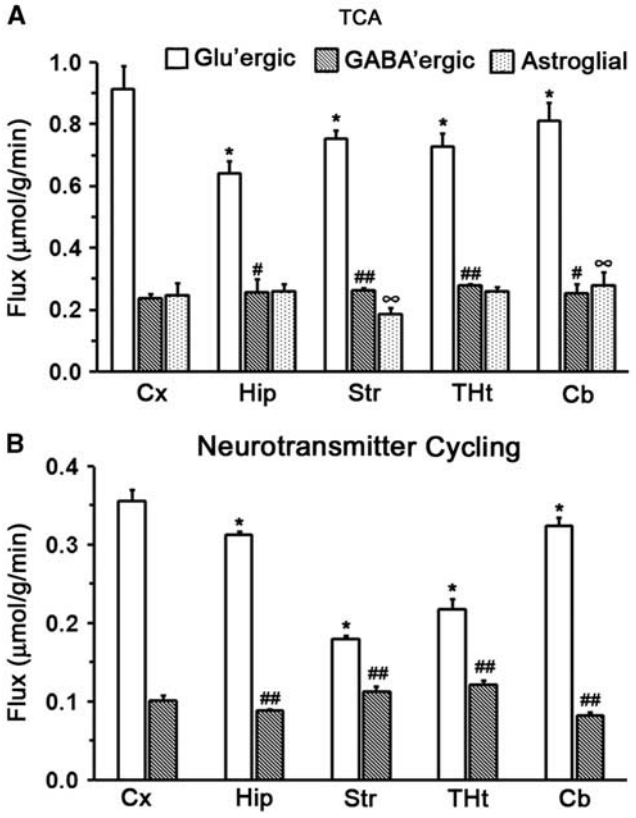


**Figure 6.** Cerebral metabolic rates in different regions of the mouse brain. (**A**) tricarboxylic acid (TCA) cycle flux, (**B**) Neurotransmitter cycling flux. Metabolic rates were calculated by best fit of the three-compartment metabolic model to the measured $^{13}C$ turnover of cerebral amino acids from [1,6-$^{13}C_2$]glucose. The values are mean ± s.d. $^{*}P<0.01$ glutamatergic flux; $^{\#}P<0.05$, $^{\#\#}P<0.01$ GABAergic rate; $^{\infty}P<0.01$ astroglial TCA cycle rate when compared with the corresponding cortical rate.

mouse brain. A particular region of the brain is attributed to specific function, which depends on the strength of the neuronal firing of the task associated with the brain region. Hence, the magnitude of energy consumed and neurotransmitter cycling rate is expected to vary across the brain. Usually, a particular region of the brain is affected in a given neurological condition. Hence, the understanding of neurotransmitter energetics across the brain may be useful for the diagnosis of the disease and to understand the disease manifestation during the treatment. In the present study, the three-compartment metabolic model was extended in mice to quantify the glutamatergic and GABAergic TCA cycle and neurotransmitter cycle rates in different regions of the mouse brain. To the best of our knowledge, this is the first comprehensive study that has evaluated the glutamatergic and GABAergic TCA cycle and neurotransmitter cycle flux across the brain of young adult mice. Our findings indicate that both the glutamatergic and GABAergic TCA cycle and neurotransmitter cycle rates are very distinct across different brain regions.

### Neurochemical Profile in the Mouse Brain

Neurochemical profile has been extensively evaluated in the rat brain using *ex vivo* and *in vivo* $^1$H NMR spectroscopy.[15,21,22] These studies have indicated inter-regional variability in the level of neurometabolites. Measurement of neurochemical profile across mouse brain has been challenging owing to the small size of the brain. However, recently, mouse brain $^1$H MR spectroscopy has gained momentum because of the improvement in NMR hardware and increased availability of genetically engineered mice for the investigation of different human diseases. A range of values has been reported for cortical Glu (10.3 to 12.4 $\mu$mol/g), GABA (1.8 to 2.0 $\mu$mol/g), NAA (8.2 to 9.2 $\mu$mol/g), Ins (4.2 to 4.6 $\mu$mol/g), and other metabolites.[23–26] In the present study, the level of cortical Glu (13.8 $\mu$mol/g), GABA (2.4 $\mu$mol/g), NAA (8.1 $\mu$mol/g), and Ins (6.5 $\mu$mol/g) is slightly higher than *in vivo* values, but significantly lower than *ex vivo* values.[27] Although absolute levels of metabolites are reported to vary across different studies, there seems to be a specific pattern for variation in the level of neurometabolites across the brain. Our data indicate that Glu level decreases in the following order: the cerebral cortex > hippocampus > striatum ~ thalamus–hypothalamus > cerebellum. The level of GABA was found to increase in the following order: cerebral cortex ~ cerebellum > hippocampus > striatum > thalamus–hypothalamus. The observed patterns of variation in the level of neurometabolite across the brain were found to be in agreement with the previous *in vivo* studies in mice.[24–26]

Glu and NAA levels were found to be highest in the cortical region, indicating more excitatory synapses and density of neurons in the cerebral cortex. The finding of higher level of Glu in the cortical region is consistent with earlier reports, which stated that the excitatory synapses outnumber the inhibitory synapses in the cerebral cortex.[28,29] Higher level of GABA in the thalamus–hypothalamus and striatum may be due to higher density of GABAergic neurons/synapses in these regions. Indeed, the hypothalamus and striatum in rats have been shown to have higher densities of GABAergic neurons when compared with other brain regions.[30] Nuclear magnetic resonance studies have also suggested a higher value of GABA in the hypothalamus when compared with other brain regions.[15,25] The level of inositol is comparatively higher in the striatal and thalamic regions, suggesting that these regions may have a higher astroglial population.

### The Metabolic Model

The metabolic model used for the analysis of the $^{13}C$ turnover data in the present study is the same as that used in the rat brain.[4] The model is well parameterized for rat cerebral cortex and has not yet been tested for other brain regions, which may have different proportions of cellular population. Glutamate, GABA, Gln, and aspartate (Asp) are readily labeled from [1,6-$^{13}C_2$]glucose or [2-$^{13}C$]acetate in different regions of the mouse brain, indicating that trafficking of neurotransmitters, Glu and GABA, between neurons and astrocytes is operational across the mouse brain. The total pool of Glu, GABA, Gln, and Asp was measured across different brain regions in the present study. Astroglial Glu pool size, an important parameter of the model, was determined using a short-time infusion of [2-$^{13}C$]acetate. Similar to rat brain, GABA and Gln were assumed to be localized exclusively in GABAergic neurons and astrocytes, respectively. The pool size of $\alpha$-ketoglutarate and oxaloacetate was the same as that in Patel *et al*.[4]

### Glucose Metabolism and Neurotransmitter Cycling in the Cerebral Cortex

Over the past two decades, glucose metabolism and neurotransmitter cycle have been studied in rat[4,7–10] and human brain.[11–13] It has been well established that cerebral metabolic rates depend on the type and dose of anesthetics used, which affect the brain activity.[5,17] Urethane (1.5 mg/kg) may be treated as a light anesthetic; hence, studies conducted under light anesthetics or awake conditions are considered for further discussion. A very recent study conducted in an awake rat has indicated cortical glucose oxidation in the range of 0.45 to 0.55 $\mu$mol/g per minute.[15] However, another study conducted in the whole brain

has reported a very high value (0.91 $\mu$mol/g per minute) for neuronal glucose oxidation.[31] Moreover, a three-compartment modeling of $^{13}C$ turnover of amino acids from glucose in halothane-anesthetized rat has revealed the rate of total (glutamatergic + GABAergic) neuronal glucose oxidation to be 0.60 $\mu$mol/g per minute.[4] The total neuronal glucose oxidation, $0.55 \pm 0.04$ $\mu$mol/g per minute ($1.11 \pm 0.07 \div 2$), obtained in the present study in mouse cerebral cortex was found to be lower than the reported value under awake conditions;[31] however, it is very close to the rates in halothane-anesthetized rats.[4]

In an awake rat cortex, total neurotransmitter cycling flux has been reported to be in the range from 0.47 to 0.57 $\mu$mol/g per minute.[15,31] The total cortical neurotransmitter cycling has been reported to be 0.57 $\mu$mol/g per minute in halothane-anesthetized rat.[4] Our finding of total neurotransmitter cycle flux ($0.45 \pm 0.03$ $\mu$mol/g per minute) in the mice cerebral cortex was found to be in good agreement with these values. In the rat cerebral cortex, neurotransmitter cycle flux has been reported to be 80% of the neuronal glucose oxidation.[5,17] In the present study, neurotransmitter cycle rate was found to be $\sim$83% of the neuronal glucose oxidation, suggesting that in the mouse cortex also most of the energy is used for supporting the processes associated with neurotransmission.

### Glucose Metabolism and Neurotransmitter Cycling in Different Brain Regions

Until now, most of the regional cerebral metabolic studies have been carried out in rats,[15,32] and very little information is available for regional glucose metabolism and neurotransmitter cycling flux in brain of mice. The $^{14}C$ deoxyglucose measurements of cerebral glucose utilization has indicated a decrease in the local glucose consumption in the following order: cerebral cortex > thalamus–striatum > hippocampus.[14] The $^{13}C$ NMR study in rats has indicated that glucose oxidation and neurotransmitter cycle flux decreased in the order of cerebral cortex > corpus callosum > subcortex in rat brain,[7] suggesting that total glucose oxidation and neurotransmitter cycle might decrease in the order of cortex > striatum $\sim$ thalamus > hippocampus. Moreover, glucose oxidation was reported to decrease in the order of cerebral cortex > striatum $\sim$ cerebellum $\sim$ hippocampus > thalamus–hypothalamus in rats in awake condition.[15] Our data indicate that neuronal glucose oxidation in the mouse brain decreases in the order of cerebral cortex > cerebellum > striatum $\sim$ thalamus–hypothalamus > hippocampus (Supplementary Table 3S). The slight variation in the pattern of metabolic flux in the current study may be due to differences in the animal species studied.

### Contribution of Excitatory and Inhibitory Fluxes in Different Regions of the Brain

The contribution of GABA to total neurotransmission and neuronal glucose oxidation has been evaluated in anesthetized rat cortex. The glucose oxidation by glutamatergic and GABAergic neurons in rat cerebral cortex under halothane anesthesia was 0.50 and 0.11 $\mu$mol/g per minute, respectively, and the corresponding neurotransmitter cycle fluxes were 0.45 and 0.14 $\mu$mol/g per minute, respectively.[4] The contribution of GABA to total neuronal glucose oxidation and neurotransmitter cycling fluxes was estimated to be 18% and 23%, respectively.[4,6] The present study indicates that the contribution of GABA to total neuronal TCA cycle is 21% (glutamatergic 0.91; GABAergic 0.24 $\mu$mol/g per minute), whereas it is 22% (glutamatergic 0.36 $\mu$mol/g per minute; GABAergic 0.10 $\mu$mol/g per minute) for the neurotransmitter cycle in mouse cerebral cortex, which is similar to the values reported in rat cortex. Further, our findings also indicate that the contribution of GABA to neurotransmitter cycle flux increases in the order of cerebellum (20%) < cerebral cortex (22%) $\sim$ hippocampus (22%) < thalamus–hypothalamus (36%) < striatum (39%) (Figure 6B, Supplementary Table 3S). The glutamatergic neurotransmission increases in the following order: striatum < thalamus–hypothalamus < hippocampus < cerebellum < cerebral cortex (Figure 6A). The finding of maximum contribution of GABA to neurotransmitter cycling in striatum and thalamus is in good agreement with the higher density of GABAergic neurons in these regions.[30,33]

Neurons and astrocytes function in a coordinated manner to achieve optimum brain functions. The total energy demand of the brain to carry out neurotransmitter activity is the sum total of TCA cycle flux of neurons and astrocytes. The data from the present study revealed that astroglial TCA cycle flux was highest in the hippocampus (22%; $V_{TCA(A)}$ 0.26 $\mu$mol/g per minute, $V_{TCA(Glu)}$ 0.64 $\mu$mol/g per minute, $V_{TCA(GABA)}$ 0.26 $\mu$mol/g per minute), followed by the cerebellum (21%) $\sim$ thalamus–hypothalamus (21%) > cerebral cortex (18%) > striatum (16%).

### Implications for Functional Neuroimaging

Traditionally, functional studies using fMRI and PET were concerned with the energy requirement of excitatory neurons.[34,35] Inhibition of the human motor cortex evoked no measurable changes in the blood-oxygenation-level-dependent signal in the no-go condition, indicating that inhibition is less metabolically demanding.[36] However, energy budget analysis has suggested that the energetic requirement for inhibitory neurons may be similar to its excitatory counterpart.[37] Recently, the relationship between baseline GABA levels and functional signal in human visual cortex has been investigated.[38] The finding indicates that blood-oxygenation-level-dependent fMRI signal is inversely correlated with baseline GABA levels, thus predicting that the functional response in the thalamus, where GABA level is significantly higher than other brain regions, will be lesser. *In vivo* studies showing increased $^{14}C_2$-deoxyglucose uptake in areas densely populated by inhibitory synapses during selective stimulation of inhibitory pathways further strengthens the hypothesis of similar energetics requirement for excitatory and inhibitory neurons.[39] The high energy demand for inhibitory synapses has been further established by the observation of rise in local field potentials and cerebral blood flow during simultaneous stimulations of the inhibitory parallel fibers and excitatory climbing fibers in cerebellar neurons.[40] In the rat cerebral cortex, inhibitory and excitatory neurons are estimated to be 15 to 30% and 70 to 85% of total neurons, respectively. Further, studies in rat[4,6] and mouse cerebral cortex (present study) indicated that GABAergic neurons account for $\sim$20% of neuronal TCA cycle flux. Moreover, the GABAergic rate has been shown to increase from isoelectricity to higher activity.[4] The current data indicate that the contribution of GABA to neurotransmitter activity increases from cerebellum (20%) < cerebral cortex (22%) $\sim$ hippocampus (22%) < thalamus–hypothalamus (36%) < striatum (39%). Hence, a selective activation of inhibitory neurons is expected to result in a higher functional signal in the striatal and thalamic regions and a least functional signal in the cerebellum and cerebral cortex. The functional output due to the stimulation of inhibitory synapses in other brain regions will be in between the cerebellum and the striatum. However, the magnitude of the functional signal in a given brain region and paradigm will depend on the collective response of the excitatory and inhibitory synapses to the stimulus.

### Limitations

The metabolic analysis carried out in the current study involves macrostructures such as the cerebral cortex, cerebellum, hippocampus, hypothalamus–thalamus, and striatum. It will be interesting to study the metabolic fluxes in microstructures such as the amygdala and substantia nigra, which are involved in different disorders such as addictions and Parkinson's disease. The

astroglial Glu pool was estimated using a strategy of short-time infusion of [2-$^{13}$C]acetate. The estimation of astroglial Glu pool involves the assumption that $^{13}$C label is not transferred from astroglial Gln to neuronal Glu. However, small leakage of $^{13}$C label into neurons cannot be ruled out. Furthermore, assumption of the labeling of glial Glu pool equal to Gln may also not be fully valid in a short-time infusion. Hence, the fraction of astroglial Glu pool obtained by Equation (2) will be overestimated to the extent that the $^{13}$C label is transferred into neuronal Glu.

## CONCLUSION

Our findings reveal that the metabolite levels are very different across the various regions of the mouse brain. Cortical regions exhibited the highest level of Glu and NAA, which shows a higher number of excitatory neurons and density, whereas the thalamic and striatal regions exhibited higher GABAergic density. The finding of higher $^{13}$C labeling of cerebral amino acids from glucose than acetate is consistent with the view of glucose as the preferred energy substrate for the brain than acetate. The neurotransmitter cycle in the mouse brain was found to decrease in the order of cerebral cortex > cerebellum > hippocampus > thalamus–hypothalamus > striatum. Glutamatergic activity was found to be highest in the cerebral cortex, whereas the GABAergic activity was observed to be maximum in the subcortical regions. To the best of our knowledge, the present investigation is the first comprehensive study that has evaluated the glutamatergic and GABAergic TCA cycle and neurotransmitter cycle fluxes across different regions of the mouse brain. These findings indicate that both the glutamatergic and GABAergic TCA cycle and neurotransmitter cycle rates are very distinct across different brain regions.

## DISCLOSURE/CONFLICT OF INTEREST

The authors declare no conflict of interest.

## ACKNOWLEDGEMENTS

We thank Dr Robin A de Graff and Dr Graeme Mason, Yale University for providing the POCE sequence and CWave software, respectively, Dr M Jerald Mahesh Kumar for providing animals in good health, Mr Bhargidhar Babu for his assistance in conducting animal study, Mr KS Varadarajan for his help with NMR experiments, Dr C Suguna for help with statistical analysis, and Dr Yamini Asthana for the critical editing of the manuscript.

## REFERENCES

1 Ottersen OP, Storm-Mathisen J. Excitatory amino acid pathways in the brain. *Adv Exp Med Biol* 1986; **203**: 263–284.
2 Schmidt WJ, Bubser M, Hauber W. Behavioural pharmacology of glutamate in the basal ganglia. *J Neural Transm Suppl* 1992; **38**: 65–89.
3 Sanacora G, Gueorguieva R, Epperson CN, Wu YT, Appel M, Rothman DL *et al.* Subtype-specific alterations of gamma-aminobutyric acid and glutamate in patients with major depression. *Arch Gen Psychiatry* 2004; **61**: 705–713.
4 Patel AB, De Graaf RA, Mason GF, Rothman DL, Shulman RG, Behar KL. The contribution of GABA to glutamate/glutamine cycling and energy metabolism in the rat cortex *in vivo*. *Proc Natl Acad Sci USA* 2005; **102**: 5588–5593.
5 Sibson NR, Dhankhar A, Mason GF, Rothman DL, Behar KL, Shulman RG. Stoichiometric coupling of brain glucose metabolism and glutamatergic neuronal activity. *Proc Natl Acad Sci USA* 1998; **95**: 316–321.
6 Chowdhury GM, Patel AB, Mason GF, Rothman DL, Behar KL. Glutamatergic and GABAergic neurotransmitter cycling and energy metabolism in rat cerebral cortex during postnatal development. *J Cereb Blood Flow Metab* 2007; **27**: 1895–1907.
7 de Graaf RA, Mason GF, Patel AB, Rothman DL, Behar KL. Regional glucose metabolism and glutamatergic neurotransmission in rat brain *in vivo*. *Proc Natl Acad Sci USA* 2004; **101**: 12700–12705.
8 Duarte JM, Lanz B, Gruetter R. Compartmentalized cerebral metabolism of [1,6-(13)C]glucose determined by *in vivo* (13)C NMR spectroscopy at 14.1 T. *Front Neuroenergetics* 2011; **3**: 3.
9 Patel AB, de Graaf RA, Rothman DL, Behar KL, Mason GF. Evaluation of cerebral acetate transport and metabolic rates in the rat brain *in vivo* using $^{1}$H-[$^{13}$C]-NMR. *J Cereb Blood Flow Metab* 2010; **30**: 1200–1213.
10 Xin L, Mlynarik V, Lanz B, Frenkel H, Gruetter R. 1H-[13C] NMR spectroscopy of the rat brain during infusion of [2-13C] acetate at 14.1 T. *Magn Reson Med* 2010; **64**: 334–340.
11 Boumezbeur F, Mason GF, de Graaf RA, Behar KL, Cline GW, Shulman GI *et al.* Altered brain mitochondrial metabolism in healthy aging as assessed by in vivo magnetic resonance spectroscopy. *J Cereb Blood Flow Metab* 2010; **30**: 211–221.
12 Gruetter R, Seaquist ER, Ugurbil K. A mathematical model of compartmentalized neurotransmitter metabolism in the human brain. *Am J Physiol Endocrinol Metab* 2001; **281**: E100–E112.
13 Shen J, Petersen KF, Behar KL, Brown P, Nixon TW, Mason GF *et al.* Determination of the rate of the glutamate/glutamine cycle in the human brain by in vivo 13C NMR. *Proc Natl Acad Sci USA* 1999; **96**: 8235–8240.
14 Eintrei C, Sokoloff L, Smith CB. Effects of diazepam and ketamine administered individually or in combination on regional rates of glucose utilization in rat brain. *Br J Anaesth* 1999; **82**: 596–602.
15 Wang J, Jiang L, Jiang Y, Ma X, Chowdhury GM, Mason GF. Regional metabolite levels and turnover in the awake rat brain under the influence of nicotine. *J Neurochem* 2010; **113**: 1447–1458.
16 Fitzpatrick SM, Hetherington HP, Behar KL, Shulman RG. The flux from glucose to glutamate in the rat brain in vivo as determined by $^{1}$H-observed, $^{13}$C-edited NMR spectroscopy. *J Cereb Blood Flow Metab* 1990; **10**: 170–179.
17 Patel AB, de Graaf RA, Mason GF, Kanamatsu T, Rothman DL, Shulman RG *et al.* Glutamatergic neurotransmission and neuronal glucose oxidation are coupled during intense neuronal activation. *J Cereb Blood Flow Metab* 2004; **24**: 972–985.
18 Tiwari V, Patel AB. Impaired glutamatergic and GABAergic function at early age in AbetaPPswe-PS1dE9 mice: implications for Alzheimer's disease. *J Alzheimers Dis* 2012; **28**: 765–769.
19 Mason GF, Rothman DL. Basic principles of metabolic modeling of NMR (13)C isotopic turnover to determine rates of brain metabolism in vivo. *Metab Eng* 2004; **6**: 75–84.
20 Alcolea A, Carrera J, Medina A. *A hybrid Marquadrt-simulated annealing method for solving the groundwater inverse problem. Calibration and reliability in groundwater modeling*. In:Model-CARE 999 Conference; 1999: Zu rich, Switzerland, 1999, p 157–163.
21 Hong ST, Balla DZ, Choi C, Pohmann R. Rat strain-dependent variations in brain metabolites detected by in vivo (1) H NMR spectroscopy at 16.4T. *NMR Biomed* 2011; **24**: 1401–1407.
22 Xin L, Gambarota G, Duarte JM, Mlynarik V, Gruetter R. Direct *in vivo* measurement of glycine and the neurochemical profile in the rat medulla oblongata. *NMR Biomed* 2010; **23**: 1097–1102.
23 Duarte JM, Lei H, Mlynarik V, Gruetter R. The neurochemical profile quantified by *in vivo* 1H NMR spectroscopy. *Neuroimage* 2012; **61**: 342–362.
24 Kulak A, Duarte JM, Do KQ, Gruetter R. Neurochemical profile of the developing mouse cortex determined by *in vivo* 1H NMR spectroscopy at 14.1 T and the effect of recurrent anaesthesia. *J Neurochem* 2010; **115**: 1466–1477.
25 Lei H, Poitry-Yamate C, Preitner F, Thorens B, Gruetter R. Neurochemical profile of the mouse hypothalamus using in vivo 1H MRS at 14.1T. *NMR Biomed* 2010; **23**: 578–583.
26 Tkac I, Henry PG, Andersen P, Keene CD, Low WC, Gruetter R. Highly resolved *in vivo* 1H NMR spectroscopy of the mouse brain at 9.4 T. *Magn Reson Med* 2004; **52**: 478–484.
27 Walls AB, Eyjolfsson EM, Smeland OB, Nilsen LH, Schousboe I, Schousboe A *et al.* Knockout of GAD65 has major impact on synaptic GABA synthesized from astrocyte-derived glutamine. *J Cereb Blood Flow Metab* 2010; **31**: 494–503.
28 Beaulieu C, Colonnier M. A laminar analysis of the number of round-asymmetrical and flat-symmetrical synapses on spines, dendritic trunks, and cell bodies in area 17 of the cat. *J Comp Neurol* 1985; **231**: 180–189.
29 Megias M, Emri Z, Freund TF, Gulyas AI. Total number and distribution of inhibitory and excitatory synapses on hippocampal CA1 pyramidal cells. *Neuroscience* 2001; **102**: 527–540.
30 Obrietan K, van den Pol AN. GABA neurotransmission in the hypothalamus: developmental reversal from Ca2+ elevating to depressing. *J Neurosci* 1995; **15**: 5065–5077.
31 Oz G, Berkich DA, Henry PG, Xu Y, LaNoue K, Hutson SM *et al.* Neuroglial metabolism in the awake rat brain: CO2 fixation increases with brain activity. *J Neurosci* 2004; **24**: 11273–11279.
32 de Graaf RA, Brown PB, Mason GF, Rothman DL, Behar KL. Detection of [1,6–$^{13}C_2$]-glucose metabolism in rat brain by in vivo $^{1}$H-[$^{13}$C]-NMR spectroscopy. *Magn Reson Med* 2003; **49**: 37–46.

33 Graveland GA, DiFiglia M. The frequency and distribution of medium-sized neurons with indented nuclei in the primate and rodent neostriatum. *Brain Res* 1985; **327**: 307–311.
34 Rothman DL, Behar KL, Hyder F, Shulman RG. In vivo NMR studies of the glutamate neurotransmitter flux and neuroenergetics: implications for brain function. *Annu Rev Physiol* 2003; **65**: 401–427.
35 Bonvento G, Sibson N, Pellerin L. Does glutamate image your thoughts? *Trends Neurosci* 2002; **25**: 359–364.
36 Waldvogel D, van Gelderen P, Muellbacher W, Ziemann U, Immisch I, Hallett M. The relative metabolic demand of inhibition and excitation. *Nature* 2000; **406**: 995–998.
37 Attwell D, Laughlin SB. An energy budget for signaling in the grey matter of the brain. *J Cereb Blood Flow Metab* 2001; **21**: 1133–1145.
38 Donahue MJ, Near J, Blicher JU, Jezzard P. Baseline GABA concentration and fMRI response. *Neuroimage* 2010; **53**: 392–398.
39 Ackermann RF, Finch DM, Babb TL, Engel Jr. J. Increased glucose metabolism during long-duration recurrent inhibition of hippocampal pyramidal cells. *J Neurosci* 1984; **4**: 251–264.
40 Caesar K, Gold L, Lauritzen M. Context sensitivity of activity-dependent increases in cerebral blood flow. *Proc Natl Acad Sci USA* 2003; **100**: 4239–4244.

Supplementary Information accompanies the paper on the Journal of Cerebral Blood Flow & Metabolism website (http://www.nature.com/jcbfm)